

Computed Torque Control of an Aerial Manipulation System with a Quadrotor and a 2-DOF Robotic Arm

Nebi Bulut¹, Ali Emre Turgut¹ and Kutluk Bilge Arıkan²

¹*Department of Mechanical Engineering, Middle East Technical University, Çankaya, Ankara, Turkey*

²*Department of Mechanical Engineering, TED University, Çankaya, Ankara, Turkey*

Keywords: Aerial Manipulation, Computed Torque Control, Gain Optimization, Robotics, Quadrotor.

Abstract: This paper presents the control of an aerial manipulation system with a quadrotor and a 2-DOF robotic arm by using the computed torque control method. The kinematic and dynamic model of the system is obtained by modeling the quadrotor and the robotic arm as a unified system. Then, the equation of motion of the unified system is got in the form of a standard robot dynamics equation. For the trajectory control of the system, computed torque control is used. Gains of the controller are optimized by using nonlinear least squares method. The performance and stability of the control structure are tested with a simulation case study.

1 INTRODUCTION

Unmanned air vehicles (UAVs) have already got the attention of researchers from all around the world in recent years. There are lots of researches have been conducted. Especially, UAVs with rotary wing i.e. quadrotors are the most studied ones (Kotarski, Benic, and Krznar, 2016), (Das, Lewis, Subbarao, 2009), (Sadr, Moosavian, and Zarafshan, 2014), and (Mahony, Kumar and Corke, 2012). There are certain advantages of the quadrotors such as the ability of vertical take-off and landing, staying hover position, and capability of high agility and maneuverability. In daily life, they are used for surveillance, rescue, and filming.

These days, in order to increase capabilities of the quadrotors, like carrying, painting and welding operations, researches are conducted about aerial manipulation. To obtain manipulated air vehicles, a robotic arm is added to the bottom of these vehicles. Different degrees of freedom serial robotic manipulators that are attached to the UAVs are studied (Kim, Choi, and Kim, 2013), (Caccavale, Giglio, Muscio and Pierri, 2014), and (Jimenez-Cano, Martin, Heredia, Ollero and Cano, 2013). Moreover, aerial manipulation with parallel manipulators is worked (Danko, Chaney and Oh, 2015). For manipulation purposes, cable-suspended studies are also available (Goodarzi, Lee and Lee, 2014), (Sreenath, Kumar, 2013), and (Alothman, Guo and Gu, 2017).

In literature, two main methods are followed to model the unified quadrotor manipulator system. The first approach is that kinematic and dynamic model of the quadrotor is created, then behaving robotic arm as a disturbance input to the quadrotor (Orsag, Korpela, Bogdan and Oh, 2013) and (Khalifa and Fanni, 2017). In the second method, quadrotor and robotic arm are modeled as one system (Kim, Choi and Kim, 2013) and (Caccavale, Giglio, Muscio and Pierri, 2014). For controlling the unified system different approaches have been developed. To deal with interaction forces between end-effector of the robotic arm and the environment, and disturbances, the compliance control strategy is used (Giglio, and Pierri, 2014). Also, a robust control strategy is studied for the trajectory tracking control of the aerial manipulation without effecting from the unmodelled dynamics and uncertainties (Mello, Raffo and Adorno, 2016). For the controller development, controller design stage can be divided into in terms of whether a single controller is designed or decoupled controllers are designed to control the overall system. For the unified system of robotic manipulator and quadrotor, decoupled dynamics are used to development of decoupled controller algorithms (Khalifa and Fanni, 2017). It can be seen that single controller implementation is studied by exploiting coupled equations of motion of the unified system (Kim, Choi and Kim, 2013). The other aspect of the controller design stage is whether a linear or nonlinear controller has proceeded for the stable system performance. A nonlinear model predictive controller

is studied to regulate the overall system around optimized trajectories (Garimella and Kobilarov, 2015). Also, by using the feedback linearized dynamics, linear controller (PID) implementations are available (Khalifa and Fanni, 2017).

In this paper, Lagrange-D'Alembert formulation is used to obtain the equation of motion of the unified system in the form of standard robotics equations of motion. For controlling the unified system, computed torque control with PID outer loop is designed. For the gain optimization procedure, multi-objective nonlinear least square solver of Matlab Global Optimization Toolbox is used. The ITAE (The Integral of Time multiply Absolute Error) is selected as an objective function to minimize the error between the input and the output. For simulating more realistic scenario, experimentally identified quadrotor's dc motors' transfer function and second order torque filtering transfer function for the robotic arm is implemented in the system's simulation.

This paper is organized in 5 sections. Section 1 is the introduction to this paper. Section 2 includes details about the modeling of the unified system. Section 3 consists of controller design pattern. Simulation results are presented in section 4. Finally, the discussion and conclusion of this paper take part in section 5.

2 MODELLING

2.1 Kinematics

Some of the kinematic parameters of the unified system can be seen in Figure 1. In this figure, O_i, O_b, O_1, O_2 and O_e are the origins of the reference frames of the inertial, quadrotor's body, link-1, link-2 and the end-effector of the robot arm, respectively.

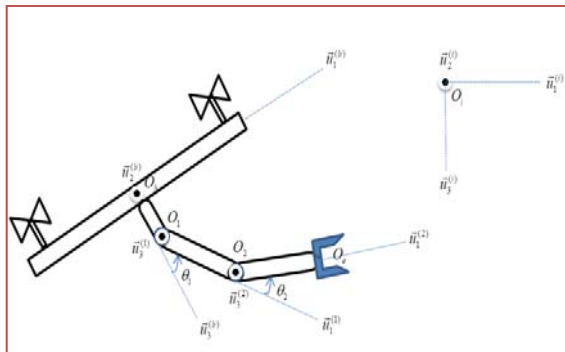


Figure 1: Side view of the unified system and some of the kinematic parameters.

Orientation of the quadrotor is designated by the set of Euler angles that are roll, pitch and yaw angles, $\bar{\gamma} = [\phi \ \theta \ \psi]^T$. Their names are phi, theta, and psi in the Latin Alphabet. By using these angles, the transformation matrix from the quadrotor's body-fixed reference frame to the earth-fixed reference frame can be written as follows,

$$\hat{C}^{(i,b)} = \begin{bmatrix} c\psi c\theta & c\psi s\theta s\phi - s\psi c\phi & c\psi s\theta c\phi + s\psi s\phi \\ s\psi c\theta & s\psi s\theta s\phi + c\psi c\phi & s\psi s\theta c\phi - c\psi s\phi \\ -s\theta & c\theta s\phi & c\theta c\phi \end{bmatrix} \quad (1)$$

In Eq. (1), $s\alpha$ and $c\alpha$ are used in place of $\sin \alpha$ and $\cos \alpha$. The table that consists of Denavit–Hartenberg parameters for the robotic arm can be given as below. Where, β_k is twist angle, θ_k is joint angle, and b_k is the offset between the joints.

Table 1: Denavit–Hartenberg Parameters.

Parameters	Link-1	Link-2
β_k	$-\frac{\pi}{2}$	0
θ_k	$\theta_1 + \frac{3\pi}{2}$	θ_2
b_k	b_1	b_2

Position of the center of the mass of the quadrotor, link-1 and link-2 of the robotic arm with respect to the inertial fixed reference frame can be written as follows,

$$\bar{p}_q^{(i)} = [x \ y \ z]^T \quad (2)$$

$$\bar{p}_1^{(i)} = \bar{p}_q^{(i)} + \hat{C}^{(i,b)} \bar{p}_1^{(b)} \quad (3)$$

$$\bar{p}_2^{(i)} = \bar{p}_q^{(i)} + \hat{C}^{(i,b)} \bar{p}_2^{(b)} \quad (4)$$

In these equations, x, y and z are Cartesian coordinates of the position of the quadrotor, $\bar{p}_q^{(i)}$, and $\bar{p}_1^{(b)}$ and $\bar{p}_2^{(b)}$ are the positions of the link-1 and link-2 in body fixed reference frame of the quadrotor.

The matrix that defines the relationship between the angular velocity of the quadrotor and time derivative of the Euler angles, \hat{L} .

$$\hat{L} = \begin{bmatrix} 1 & 0 & -s\theta \\ 0 & c\phi & c\theta s\phi \\ 0 & -s\phi & c\theta c\phi \end{bmatrix} \quad (5)$$

Then, the relation can be further written as by noticing that $\bar{w}_q^{(b)}$ is the angular velocity of the quadrotor in body fixed reference frame,

$$\bar{w}_q^{(b)} = \hat{L}\dot{\bar{Y}} \quad (6)$$

Also, further relations can be given as,

$$\bar{w}_q^{(i)} = \hat{C}^{(i,b)} \bar{w}_q^{(b)} \quad (7)$$

$$\bar{w}_q^{(i)} = \hat{C}^{(i,b)} \hat{L}\dot{\bar{Y}} = \hat{T}\dot{\bar{Y}} \quad (8)$$

Where, $\bar{w}_q^{(i)}$ is the angular velocity in the inertial fixed reference frame, and \hat{T} maps the rate of change of the Euler angles into $\bar{w}_q^{(i)}$. Overhead dot is used for the time derivative of the corresponding parameter.

Jacobian matrix, J can be used to express the linear and angular velocities of the link-1 and link-2 in quadrotor's body fixed reference frame as,

$$\dot{\bar{p}}_1^{(b)} = \hat{J}_{v1} \dot{\bar{\Omega}} \quad (9)$$

$$\dot{\bar{p}}_2^{(b)} = \hat{J}_{v2} \dot{\bar{\Omega}} \quad (10)$$

$$\bar{w}_1^{(b)} = \hat{J}_{w1} \dot{\bar{\Omega}} \quad (11)$$

$$\bar{w}_2^{(b)} = \hat{J}_{w2} \dot{\bar{\Omega}} \quad (12)$$

Then, linear and angular velocities in the inertial fixed reference frame can be written as,

$$\dot{\bar{p}}_1^{(i)} = \dot{\bar{p}}_q^{(i)} + \hat{C}^{(i,b)} \dot{\bar{p}}_1^{(b)} + \hat{C}^{(i,b)} \dot{\bar{p}}_1^{(b)} \quad (13)$$

$$\dot{\bar{p}}_2^{(i)} = \dot{\bar{p}}_q^{(i)} + \hat{C}^{(i,b)} \dot{\bar{p}}_2^{(b)} + \hat{C}^{(i,b)} \dot{\bar{p}}_2^{(b)} \quad (14)$$

$$\dot{\bar{p}}_1^{(i)} = \dot{\bar{p}}_q^{(i)} + SSM(w_q^{(b)}) \hat{C}^{(i,b)} \bar{p}_1^{(b)} + \hat{C}^{(i,b)} \hat{J}_{v1} \dot{\bar{\Omega}} \quad (15)$$

$$\dot{\bar{p}}_2^{(i)} = \dot{\bar{p}}_q^{(i)} + SSM(w_q^{(b)}) \hat{C}^{(i,b)} \bar{p}_2^{(b)} + \hat{C}^{(i,b)} \hat{J}_{v2} \dot{\bar{\Omega}} \quad (16)$$

$$\bar{w}_1^{(i)} = \bar{w}_q^{(i)} + \hat{C}^{(i,b)} \hat{J}_{w1} \dot{\bar{\Omega}} \quad (17)$$

$$\bar{w}_2^{(i)} = \bar{w}_q^{(i)} + \hat{C}^{(i,b)} \hat{J}_{w2} \dot{\bar{\Omega}} \quad (18)$$

SSM is used for skew-symmetric operation. Generalized coordinates and velocities of the unified system can be defined as,

$$\bar{q} = [x \quad y \quad z \quad \phi \quad \theta \quad \psi \quad \theta_1 \quad \theta_2]^T \quad (19)$$

$$\dot{\bar{q}} = [\dot{x} \quad \dot{y} \quad \dot{z} \quad \dot{\phi} \quad \dot{\theta} \quad \dot{\psi} \quad \dot{\theta}_1 \quad \dot{\theta}_2]^T$$

By using linear and angular velocity influence coefficients, \hat{V} and \hat{W} , respectively, and Eq. (19), the linear and angular velocities can be written further as (Ozgoren, 2017),

$$\dot{\bar{p}}_q^{(i)} = \begin{bmatrix} \hat{I}_{3 \times 3} & \hat{0}_{3 \times 5} \end{bmatrix} \dot{\bar{q}} = \hat{V}_q \dot{\bar{q}} \quad (20)$$

$$\bar{w}_q^{(i)} = \begin{bmatrix} \hat{0}_{3 \times 3} & \hat{T} & \hat{0}_{3 \times 2} \end{bmatrix} \dot{\bar{q}} = \hat{W}_q \dot{\bar{q}} \quad (21)$$

$$\dot{\bar{p}}_1^{(i)} = \begin{bmatrix} \hat{I}_{3 \times 3} & -SSM(\hat{C}^{(i,b)} \bar{p}_1^{(b)}) \hat{T} & \hat{C}^{(i,b)} \hat{J}_{v1} \end{bmatrix} \dot{\bar{q}} = \hat{V}_1 \dot{\bar{q}} \quad (22)$$

$$\dot{\bar{p}}_2^{(i)} = \begin{bmatrix} \hat{I}_{3 \times 3} & -SSM(\hat{C}^{(i,b)} \bar{p}_2^{(b)}) \hat{T} & \hat{C}^{(i,b)} \hat{J}_{v2} \end{bmatrix} \dot{\bar{q}} = \hat{V}_2 \dot{\bar{q}} \quad (23)$$

$$\bar{w}_1^{(i)} = \begin{bmatrix} \hat{0}_{3 \times 3} & \hat{T} & \hat{C}^{(i,b)} \hat{J}_{w1} \end{bmatrix} \dot{\bar{q}} = \hat{W}_1 \dot{\bar{q}} \quad (24)$$

$$\bar{w}_2^{(i)} = \begin{bmatrix} \hat{0}_{3 \times 3} & \hat{T} & \hat{C}^{(i,b)} \hat{J}_{w2} \end{bmatrix} \dot{\bar{q}} = \hat{W}_2 \dot{\bar{q}} \quad (25)$$

2.2 Dynamics

Equation of motion of the unified system is obtained by using the following form of the Lagrange-D'Alembert formulation.

$$\frac{d}{dt} \left(\frac{\partial L}{\partial \dot{\bar{q}}} \right) - \frac{\partial L}{\partial \bar{q}} = \bar{u} + \bar{u}_{ext} \quad (26)$$

$$L = K - U$$

In Eq. (26), K is the total kinetic energy and U is the total potential energy of the unified system, and L is the Lagrange operator. Also, \bar{u} and \bar{u}_{ext} are the generalized input force and interaction force between end-effector and the environment, respectively.

2.2.1 Kinetic and Potential Energies

The total kinetic energy of the overall system is the sum of the kinetic energies of the quadrotor body with mass m_b , link-1 with mass m_1 , and link-2 with mass m_2 .

$$K = K_b + K_1 + K_2 \quad (27)$$

$$K_b = \frac{1}{2} \dot{\bar{p}}_q^{(i)T} m_b \dot{\bar{p}}_q^{(i)} + \frac{1}{2} \bar{\omega}_q^{(i)T} \hat{C}^{(i,b)} \hat{I}_b \hat{C}^{(i,b)T} \bar{\omega}_q^{(i)} \quad (28)$$

$$K_1 = \frac{1}{2} \dot{\bar{p}}_1^{(i)T} m_1 \dot{\bar{p}}_1^{(i)} + \frac{1}{2} \bar{\omega}_1^{(i)T} \hat{C}^{(i,b)} \hat{C}^{(b,1)} \hat{I}_1 \hat{C}^{(b,1)T} \hat{C}^{(i,b)T} \bar{\omega}_1^{(i)} \quad (29)$$

$$K_2 = \frac{1}{2} \dot{\bar{p}}_2^{(i)T} m_2 \dot{\bar{p}}_2^{(i)} + \frac{1}{2} \bar{\omega}_2^{(i)T} \hat{C}^{(i,b)} \hat{C}^{(b,2)} \hat{I}_2 \hat{C}^{(b,2)T} \hat{C}^{(i,b)T} \bar{\omega}_2^{(i)} \quad (30)$$

In the above equations, I is the constant inertia matrix in the corresponding body fixed reference frames.

Similarly, potential energies of each mass elements as follows,

$$U = U_b + U_1 + U_2 \quad (31)$$

$$U_b = m_b g \bar{u}_3^T \bar{p}_q^{(i)} \quad (32)$$

$$U_1 = m_1 g \bar{u}_3^T \bar{p}_1^{(i)} \quad (33)$$

$$U_2 = m_2 g \bar{u}_3^T \bar{p}_2^{(i)} \quad (34)$$

In these equations, g is the gravity.

2.2.2 Equation of Motion

By plugging Eq. (31) and Eq. (27) into Eq. (26), following equation of motion of the unified system is obtained.

$$\hat{M}(\bar{q})\ddot{\bar{q}} + \hat{C}(\bar{q}, \dot{\bar{q}})\dot{\bar{q}} + \hat{G}(\bar{q}) = \bar{u} + \bar{u}_{ext} \quad (35)$$

In above equation, \hat{M} is the positive definite inertia matrix, \hat{C} includes centripetal, Coriolis and gyroscopic terms, and gravity terms take part in matrix \hat{G} . To calculate inertia matrix, following kinetic energy formulation is used (Siciliano, Sciavicco, Villani and Oriolo, 2009).

$$K = \frac{1}{2} \dot{\bar{q}}^T \hat{M}(\bar{q}) \dot{\bar{q}} \quad (36)$$

Inertia matrix can be further written by using Eq. (36) and from Eq. (20) to Eq. (25) as

$$\hat{M}(\bar{q}) = \hat{V}_q^T m_b \hat{V}_q + \hat{W}_q^T \hat{C}^{(i,b)} \hat{I}_b \hat{C}^{(i,b)T} \hat{W}_q \quad (37)$$

$$+ \sum_{k=1}^2 \hat{V}_k^T m_k \hat{V}_k + \hat{W}_k^T (\hat{C}^{(i,b)} \hat{C}^{(b,k)}) \hat{I}_k (\hat{C}^{(i,b)} \hat{C}^{(b,k)})^T \hat{W}_k$$

Also, elements of the \hat{C} can be calculated by using following relation (Siciliano, Sciavicco, Villani and Oriolo, 2009),

$$c_{a,b} = \sum_{j=1}^8 \frac{1}{2} \left\{ \frac{\partial m_{a,b}}{\partial q_j} + \frac{\partial m_{a,j}}{\partial q_b} - \frac{\partial m_{j,b}}{\partial q_a} \right\} \quad (38)$$

Finally, the column matrix \hat{G} is given as,

$$\hat{G}(\bar{q}) = \frac{\partial U}{\partial \bar{q}} \quad (39)$$

Generalized input force, \bar{u} and interaction force that is applied on the tip point of the end-effector, \bar{u}_{ext} are obtained by using virtual work principle.

$$\bar{u} = \hat{H} \begin{bmatrix} \bar{f}_q^{(b)} \\ \bar{\tau}_q^{(b)} \\ \bar{\tau}_{12} \end{bmatrix} \quad (40)$$

$$\bar{u} = \begin{bmatrix} \hat{C}^{(i,b)} & \hat{0}_{3 \times 3} & \hat{0}_{3 \times 2} \\ \hat{0}_{3 \times 3} & \hat{I} & \hat{0}_{3 \times 2} \\ \hat{0}_{2 \times 3} & \hat{0}_{2 \times 3} & \hat{I}_{2 \times 2} \end{bmatrix} \begin{bmatrix} \bar{f}_q^{(b)} \\ \bar{\tau}_q^{(b)} \\ \bar{\tau}_{12} \end{bmatrix} \quad (41)$$

$$u_{ext} = \begin{bmatrix} \hat{I}_{3 \times 3} & \hat{0}_{3 \times 3} \\ SSM(\bar{p}_e^{(b)}) & \hat{I}_{3 \times 3} \\ \hat{J}_{ve}^T & \hat{J}_{we}^T \end{bmatrix} \bar{P} \quad (42)$$

In Eq. (40),

$$\det(\hat{H}) = \cos(\theta) \quad (43)$$

Therefore, if $\theta \neq \pi n - \frac{\pi}{2}$, $n \in Z$,

Then, \hat{H} is an invertible square matrix. In this study, this condition is satisfied.

Where $*_x*$ is used to show sizes of matrices. $\bar{p}_e^{(b)}$ is the position of the end-effector's tip point in the quadrotor's body-fixed reference frame. Also, \hat{J} is the Jacobian matrix of the end-effector. Forces and torques that are generated by the quadrotor's dc motors are $\bar{f}_q^{(b)}$ and $\bar{\tau}_q^{(b)}$, respectively. In addition to that, the generated torques by the arm joints are $\bar{\tau}_{12}$. Moreover, \bar{P} is the column matrix of applied forces and moments on the end-effector's tip point.

$$\bar{f}_q^{(b)} = [0 \quad 0 \quad f_z]^T, \quad \bar{\tau}_q^{(b)} = [\tau_{q1} \quad \tau_{q2} \quad \tau_{q3}]^T \quad (44)$$

$$\bar{P} = [F_1 \quad F_2 \quad F_3 \quad M_1 \quad M_2 \quad M_3]^T \quad (45)$$

Relationship between quadrotor's dc motors rotational speed and the generated force and torques by the quadrotor's motor are written in Eq. (46). Where c_r and c_d are dc motor's thrust and drag coefficients.

$$\begin{bmatrix} f_z \\ \tau_{q1} \\ \tau_{q2} \\ \tau_{q3} \end{bmatrix} = \begin{bmatrix} -c_r & -c_r & -c_r & -c_r \\ 0 & -dc_r & 0 & dc_r \\ dc_r & 0 & -dc_r & 0 \\ -c_d & c_d & -c_d & c_d \end{bmatrix} \begin{bmatrix} \omega_1^2 \\ \omega_2^2 \\ \omega_3^2 \\ \omega_4^2 \end{bmatrix} \quad (46)$$

Where, f_z is the sum of the total thrust generated by the quadrotor's rotors.

For the transfer function between commanded rotational speed of the quadrotor's dc motor and achieved rotational speed, following transfer function that is obtained by the Yildiz, 2015 is used.

$$G(s) = \frac{\text{Achieved_Rotor_Speed}}{\text{Commanded_Rotor_Speed}} = \frac{0.98}{0.062s+1} \quad (47)$$

It is assumed that arm joints' servo motors are getting torque input from the controller. Instead of directly applying the controller torque inputs to the joints, commanded torques are filtering by using a

second order filter in the following form with $\zeta = 0.707$ and $w_n = 20$ Hz.

$$G(s) = \frac{w_n^2}{s^2 + 2\zeta w_n s + w_n^2} \quad (48)$$

3 CONTROLLER DESIGN

To control the overall system, computed torque control with PID outer loop is designed. Control architecture of the unified system can be seen in Figure 2.

Following control input is selected to control the overall system while $\bar{u}_{cur} = 0$.

$$\bar{u} = \hat{M}(\bar{q})v + \hat{C}(\bar{q}, \dot{\bar{q}})\dot{\bar{q}} + \bar{G}(\bar{q}) \quad (49)$$

Then, substituting this control law into Eq. (35), it follows that,

$$\ddot{\bar{q}} = v \quad (50)$$

After this control input, complicated nonlinear controller design turns into a simpler design problem. Then, v can be selected as,

$$v = \ddot{\bar{q}}_d + \hat{K}_p \bar{e} + \hat{K}_d \dot{\bar{e}} + K_i \int_0^t \bar{e}(\tau) d\tau \quad (51)$$

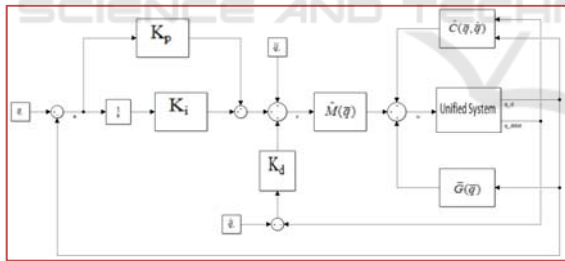


Figure 2: Control architecture of the overall system.

Hence, the overall control input is written as,

$$\bar{u} = \hat{M}(\bar{q})(\ddot{\bar{q}}_d + \hat{K}_p \bar{e} + \hat{K}_d \dot{\bar{e}} + K_i \int_0^t \bar{e}(\tau) d\tau) + \hat{C}(\bar{q}, \dot{\bar{q}})\dot{\bar{q}} + \bar{G}(\bar{q}) \quad (52)$$

Where \hat{K}_p , \hat{K}_d and \hat{K}_i are the positive definite diagonal gain matrices.

Then, the resulting error dynamics can be written as,

$$\ddot{\bar{e}} + \hat{K}_p \bar{e} + \hat{K}_d \dot{\bar{e}} + K_i \int_0^t \bar{e}(\tau) d\tau = 0 \quad (53)$$

According to linear system theory, convergence of the tracking error to zero is guaranteed (Siciliano and Khatib, 2008).

Note 1: $\ddot{\bar{q}}_d$ can be calculated numerically, but it causes derivative noises. In simulations it is assumed to be zero.

3.1 Quadrotor Position Control

By using Eq. (49), to control the quadrotor's position following expression can be written. In this equation, subscripts are used to show the corresponding indices of the matrices. However, Eq. (54) requires the desired roll and pitch angles. In this stage, they are not available.

$$\begin{bmatrix} u_1 \\ u_2 \\ u_3 \end{bmatrix} = [\hat{M}(\bar{q})]_{(1:3,1:3)} v + [\hat{C}(\bar{q}, \dot{\bar{q}})]_{(1:3,1:3)} \dot{\bar{q}} + [\bar{G}(\bar{q})]_{(1:3)} \quad (54)$$

To cope with this problem, following modified form of the inertia matrix is used.

$$\hat{M}(\bar{q}) = \begin{bmatrix} * & * & * & 0 & 0 & * & * & * \\ * & * & * & 0 & 0 & * & * & * \\ * & * & * & 0 & 0 & * & * & * \\ * & * & * & * & * & * & * & * \\ * & * & * & * & * & * & * & * \\ * & * & * & * & * & * & * & * \\ * & * & * & * & * & * & * & * \\ * & * & * & * & * & * & * & * \end{bmatrix} \quad (55)$$

First three elements of the columns four and five are replaced by the zero. By this way, the requirement of the knowledge of the desired roll and pitch angles is eliminated. These elements of the inertia matrix are often negligible since robotic arm's links are much lighter than quadrotor's body (Arleo, Caccavale, Muscio and Pierri, 2013).

Then, to compute desired roll and pitch angles, from Eq. (41) and Eq. (44) following relation can be written

$$\bar{u}_{1:2:3} = \begin{bmatrix} u_1 \\ u_2 \\ u_3 \end{bmatrix} = \begin{bmatrix} (c\psi s\theta c\phi + s\psi s\phi) f_z \\ (s\psi s\theta c\phi - c\psi s\phi) f_z \\ (c\theta c\phi) f_z \end{bmatrix} \quad (56)$$

From Eq. (56)

$$f_z = \sqrt{\bar{u}_{123}^T \bar{u}_{123}} \quad (57)$$

$$\theta_{des} = \arctan\left(\frac{u_1 \cos(\psi) + u_2 \sin(\psi)}{u_3}\right) \quad (58)$$

$$\phi_{des} = \arcsin\left(\frac{u_1 \sin(\psi) - u_2 \cos(\psi)}{f_z}\right) \quad (59)$$

3.2 Quadrotor Attitude Control

From Eq. (49), following relation can be written

$$\bar{u}_{456} = \begin{bmatrix} u_4 \\ u_5 \\ u_6 \end{bmatrix} = [\hat{M}(\bar{q})]_{(46,18)} v + [\hat{C}(\bar{q}, \dot{\bar{q}})]_{(46,18)} \dot{\bar{q}} + [\bar{G}(\bar{q})]_{(46)} \quad (60)$$

Eq. (41) and Eq. (60) give the torques of the vehicle as,

$$\bar{\tau}_q^{(b)} = (\hat{L}^t)^{-1} \bar{u}_{456} \quad (61)$$

Note 2 : Quadrotor inputs that are angular speeds of the dc motors can be computed by benefiting from the Eq. (46), Eq. (44), Eq. (57) and Eq. (61).

3.3 Manipulator Joint Angles Control

From Eq. (49),

$$\bar{u}_{78} = \begin{bmatrix} u_7 \\ u_8 \end{bmatrix} = [\hat{M}(\bar{q})]_{(78,18)} v + [\hat{C}(\bar{q}, \dot{\bar{q}})]_{(78,18)} \dot{\bar{q}} + [\bar{G}(\bar{q})]_{(78)} \quad (62)$$

Eq. (41) and Eq. (62) give the torque inputs of the arm joints as,

$$\bar{\tau}_{12} = \bar{u}_{78} \quad (63)$$

3.4 Gain Optimization

Gains of the computed torque controller are optimized by using nonlinear least-squares solver of the MATLAB Global Optimization Toolbox. For the objective function, ITAE (The Integral of Time multiply Absolute Error) given in Eq. (64) is used.

$$ITAE = \int_0^T t |e(t)| dt \quad (64)$$

This is a multi-objective optimization problem since there are 8 trajectories that should be optimized at the same time.

To make the optimization faster, Simulink model of the overall system is transformed into executable

model and then, gains are tuned for the minimum trajectory errors.

4 SIMULATION RESULTS

Proposed control algorithms are tested by simulation in Matlab/Simulink environment. Table 2 shows numerical values that are used in the simulation.

Table 2: Numeric Parameters of the Unified System.

	Quadrotor	Link-1 & Link-2
Mass (kg)	2.6550	0.1700
d (m)	0.6870	0.3000
I_{xx} (kgm²)	0.0457	7.0830e-05
I_{yy} (kgm²)	0.0457	0.0013
I_{zz} (kgm²)	0.0846	0.0013

Table 3: Simulation Scenario Parameters.

Time(s)	0-9	10-19	20-25	25-60
x (m)	0-5	5	5	5
y (m)	0-3	3	3	3
z (m)	0-(-2)	-2	-2	-2
φ (deg)	-	-	-	-
θ (deg)	-	-	-	-
ψ (deg)	0	0	0	0
θ₁ (deg)	0	0-15	15	15
θ₂ (deg)	0	0-10	10	10
F₁ (N)	0	0	0-5	5
F₂ (N)	0	0	0-1	1
F₃ (N)	0	0	0-5	5

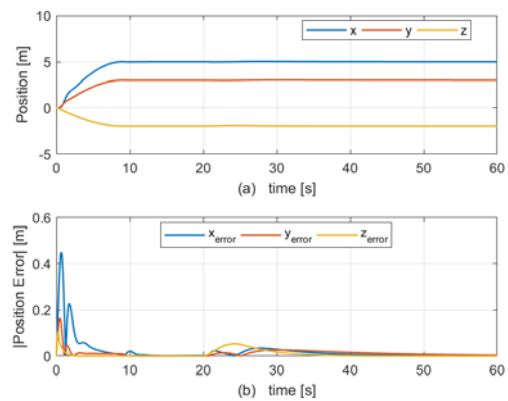


Figure 3: (a): Position of the quadrotor, (b): Absolute position error of the quadrotor.

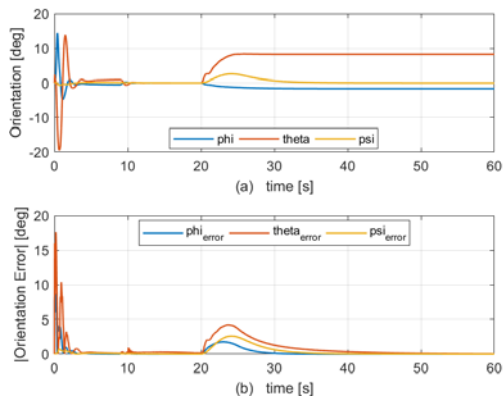


Figure 4: (a): Orientation of the quadrotor, (b): Absolute orientation error of the quadrotor.

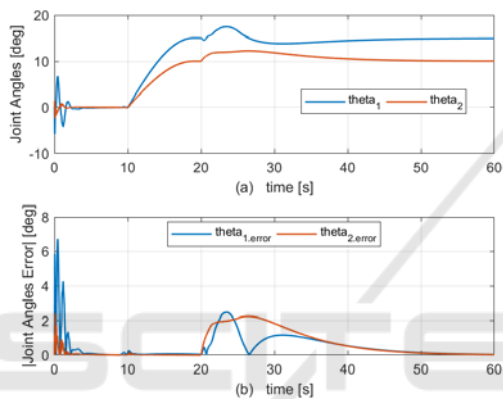


Figure 5: (a): Angular position of the joints of the robotic arm, (b): Absolute angular position error of the joints of the robotic arm.

Table 3 shows the simulated scenario parameters. From 0 to 9 seconds quadrotor positions x , y and z are commanded, and then, they are held constant through the simulation, other parameters are held as zero. Roll and pitch angles are the intermediate control inputs, and they are not directly controlled. From 10 to 19 seconds 15 degree and 10 degree joint angles are commanded to the robotic arm, and then they are commanded to stay in these angles. From 20 to 25 seconds interaction forces are applied to the tip point of the end-effector, and then they stay constant to the end of the simulation.

Figure 3 shows the achieved quadrotor position in 3-D space and the error between the desired and the achieved position. Euler angles of the quadrotor and the error between the commanded and actual Euler angles are demonstrated in Figure 4. Finally, the angular position of the robotic arm joints and the error between the desired and achieved joint angles are given in Figure 5.

5 DISCUSSION AND CONCLUSION

In this paper, an aerial manipulation system consisting of a quadrotor and a robotic arm is studied. Equation of motion of the unified system is obtained in the form of equations of standard robotic systems. Then, the computed torque controller is designed for the trajectory tracking. Gains of the controller is optimized based on minimizing the error between the input and the output states of the robotic system. The designed controller is tested in the simulation environment with the highly nonlinear dynamic model of the system in addition to quadrotor's dc motors' transfer functions and torque filters of the robot arm's joints.

From Figure 3, quadrotor is commanded to come to desired positions in 9 seconds. Then, the robotic arm is moved from 10-19 seconds to the desired position. This movement does not affect the position of the quadrotor too much. However, from 20 to 25 seconds, interaction forces are applied from the starting from the zero value and continue to apply to the end of the simulation. As a result, positions of the quadrotor are affected by the interaction forces, but the controller shows a robust behavior and brings the quadrotor to its original position. While doing this, to balance the interaction forces, quadrotor tilts and has nonzero roll and pitch angles as seen from Figure 4 starting from time = 20 seconds. This is an expected behavior since quadrotor is an underactuated vehicle, and x and y positions are coupled with the pitch and roll angles, respectively. Angular positions of the robotic arm also disturbed by the interaction forces. However, due to the controller action, joint angles settle down to their original values.

Simulation studies shows that proposed controller can achieve good trajectory tracking performance for all states, simultaneously. Also, under the action of interaction forces, it can deal with these disturbances up to some points.

REFERENCES

- Kotarski, D., Benic, Z., Krznar, M., 2016. Control Design for Unmanned Aerial Vehicles with Four Rotors. *Interdisciplinary Description of Complex Systems* 14, 236–245.
- Das, A., Lewis, F., Subbarao, K., 2009. Dynamic inversion with zero-dynamics stabilisation for quadrotor control. *IET Control Theory & Applications* 3, 303–314.

- Sadr, S., Moosavian, S. A. A., Zarafshan, P., 2014. Dynamics Modeling and Control of a Quadrotor with Swing Load. *Journal of Robotics* 2014, 1–12.
- Mahony, R., Kumar, V., Corke, P., 2012. Multirotor Aerial Vehicles: Modeling, Estimation, and Control of Quadrotor. *IEEE Robotics & Automation Magazine* 19, 20–32.
- Goodarzi, F. A., Lee, D., Lee, T., 2014. Geometric stabilization of a quadrotor UAV with a payload connected by flexible cable. 2014 American Control Conference.
- Sreenath, K., Kumar, V., 2013. Dynamics, Control and Planning for Cooperative Manipulation of Payloads Suspended by Cables from Multiple Quadrotor Robots. *Robotics: Science and Systems IX*.
- Alothman, Y., Guo, M., Gu, D., 2017. Using iterative LQR to control two quadrotors transporting a cable-suspended load. *IFAC-PapersOnLine* 50, 4324–4329.
- Kim, S., Choi, S., Kim, H. J., 2013. Aerial manipulation using a quadrotor with a two DOF robotic arm. 2013 IEEE/RSJ International Conference on Intelligent Robots and Systems.
- Caccavale, F., Giglio, G., Muscio, G., Pierri, F., 2014. Adaptive control for UAVs equipped with a robotic arm. *IFAC Proceedings Volumes* 47, 11049–11054.
- Jimenez-Cano, A., Martin, J., Heredia, G., Ollero, A., Cano, R., 2013. Control of an aerial robot with multi-link arm for assembly tasks. 2013 IEEE International Conference on Robotics and Automation.
- Danko, T. W., Chaney, K. P., Oh, P. Y., 2015. A parallel manipulator for mobile manipulating UAVs. 2015 IEEE International Conference on Technologies for Practical Robot Applications (TePRA).
- Orsag, M., Korpela, C., Bogdan, S., Oh, P., 2013. Lyapunov based model reference adaptive control for aerial manipulation. 2013 International Conference on Unmanned Aircraft Systems (ICUAS).
- Khalifa, A., Fanni, M., 2017. A new quadrotor manipulation system: Modeling and point-to-point task space control. *International Journal of Control, Automation and Systems* 15, 1434–1446.
- Giglio, G., Pierri, F., 2014. Selective compliance control for an unmanned aerial vehicle with a robotic arm. 22nd Mediterranean Conference on Control and Automation.
- Mello, L. S., Raffo, G. V., Adorno, B. V., 2016. Robust whole-body control of an unmanned aerial manipulator. 2016 European Control Conference (ECC).
- Garimella, G., Kobilarov, M., 2015. Towards model-predictive control for aerial pick-and-place. 2015 IEEE International Conference on Robotics and Automation (ICRA).
- Ozgoren, M. K., 2017. Lecture Notes for ME 522 (Principles of Robotics), Department of Mechanical Engineering, METU.
- Siciliano, B., Sciavicco, L., Villani, L., Oriolo, G., 2009. *Robotics Modelling, Planning and Control*. Springer, London.
- Yildız, M., 2015. Effects Of Active Landing Gear On The Attitude Dynamics Of A Quadrotor (thesis). Ankara.
- Siciliano, B., Khatib, O., 2008. *Springer handbook of robotics*: Springer-Verlag, New York Inc.
- Arleo, G., Caccavale, F., Muscio, G., Pierri, F., 2013. Control of quadrotor aerial vehicles equipped with a robotic arm. 21st Mediterranean Conference on Control and Automation.
- Lewis, F. L., Abdallah, C. T., Dawson, D. M., Lewis, F. L., 2018. *Robot manipulator control: theory and practice*. Lightning Source UK Ltd., Milton Keynes UK.